Molecular Vision 2022; 28:340-351 <http://www.molvis.org/molvis/v28/340>
Received 21 April 2021 | Accepted 30 September 2022 | Published 2 October 2022

Oxidative stress alters transcript localization of disease-associated genes in the retinal pigment epithelium

Tadeusz J. Kaczynski,[1,2] Elizabeth D. Au,[1] Michael H. Farkas[1,2,3]

[1]Department of Ophthalmology, State University of New York at Buffalo, Buffalo, NY; [2]Research Service, VA Medical Center, Buffalo, NY; [3]Department of Biochemistry, State University of New York at Buffalo, Buffalo, NY

Purpose: Nuclear retention is a mechanism whereby excess RNA transcripts are stored in the event that a cell needs to quickly respond to a stimulus; maintaining proper nuclear-to-cytoplasmic balance is important for cellular homeostasis and cell function. There are many mechanisms that are employed to determine whether to retain a transcript or export it to the cytoplasm, although the extent to which tissue or cell type, internal and external stressors, and disease pathogenesis affect this process is not yet clear. As the most biochemically active tissue in the body, the retina must mitigate endogenous and exogenous stressors to maintain cell health and tissue function. Oxidative stress, believed to contribute to the pathogenesis or progression of age-related macular degeneration (AMD) and inherited retinal dystrophies (IRDs), is produced both internally from biochemical processes as well as externally from environmental insult. Here, we evaluate the effect of oxidative stress on transcript localization in the retinal pigment epithelium (RPE), with specific focus on transcripts related to RPE function and disease.

Methods: We performed poly(A) RNA sequencing on nuclear and cytoplasmic fractions from human induced pluripotent stem cell–derived retinal pigment epithelium (iPSC-RPE) cells exposed to hydrogen peroxide (H_2O_2), as well as on untreated controls.

Results: Under normal conditions, the number of mRNA transcripts retained in the nucleus exceeded that found in studies on other tissues. Further, the nuclear-to-cytoplasmic ratio of transcripts was altered following oxidative stress, as was the retention of genes associated with AMD and IRDs, as well as those that are important for RPE physiology.

Conclusions: These results provide a localization catalog of all expressed mRNA in iPSC-RPE under normal conditions and after exposure to H_2O_2, shedding light on the extent to which H_2O_2 alters transcript localization and potentially offering insight into one mechanism through which oxidative stress may contribute to the progression of visual disorders.

It has long been widely accepted that mRNA is transcribed, processed, and rapidly exported from the nucleus to the cytoplasm. Given the role of mRNA in the production of proteins, it seems vital that export to the cytoplasm rapidly occurs to promote translation. This view, however, is being challenged by studies of ever-increasing sophistication [1]. On a cell-by-cell basis, transcription occurs in bursts. For any given gene, one cell may express an excess of the transcript compared to the neighboring cell. Additionally, to maintain a homeostatic environment, excess transcripts can be retained in the nucleus, some for most their lifetime [1]. Nuclear RNA retention on a global scale is a relatively new concept. It is not yet completely clear how transcripts are retained if retention differs by cell or tissue type or how stress or disease affects this process.

While nuclear retention studies are still in their infancy, some have begun to examine the role played by a variety of factors. Aberrant RNA localization can be caused by internal factors such as mutations in nuclear export factors, triplet repeat expansion, and mis-splicing, leading to intron retention [2]. These factors are implicated in a multitude of neurodegenerative diseases, such as various types of myotonic dystrophy, Huntington's disease, and glial cell tumors [3-6]. Repeat expansions in *DMPK* and *ZNF9*, which are causes of muscular dystrophy, lead to the aberrant mRNA being retained in nuclear foci [7]. Here, the mutant mRNAs recruit RNA-binding proteins, thus preventing their normal function in the cell.

External factors have also been shown to play a role in nuclear retention. Export of mRNA under normal circumstances is performed with strict quality control, but heat stress causes changes in mRNA export from the nucleus [8]. Typically, an mRNA is checked for proper splicing, capping, and polyadenylation before being exported to the cytoplasm. However, in times of heat stress, heat shock–responsive mRNAs bypass quality control checks and are rapidly exported to the cytoplasm for translation. On the other hand, the export of mRNAs that are not required to respond to the stressor is inhibited. Other external stressors remain to be studied, and little is known about the role of oxidative stress

Correspondence to: Michael H. Farkas, VA Medical Center Buffalo, 3495 Bailey Ave., Bldg 20, Rm 239, Buffalo, NY, 14214, Phone: 1 (716) 834-9200 x5638; email: mhfarkas@buffalo.edu

on mRNA export, which is specifically of note with regard to this study.

Although studies have begun to uncover a potential role for nuclear retention in disease pathogenesis, more analysis is necessary. Retinal disease is especially complex, due to genetic heterogeneity and a lack of complete understanding of both the underlying genetic components and environmental effects. Age-related macular degeneration (AMD) results in loss of retinal pigment epithelium (RPE) in the macula region of the eye, leading to death of the overlying photoreceptors and central vision loss. While no specific genetic mutations have been identified to cause AMD, 34 genetic loci have been implicated with increased risk via genome-wide association studies [9]. The genetic component of AMD accounts for as little as 37% of disease pathology, while environmental components (e.g., oxidative stress, smoking, diet) account for the remainder. Moreover, inherited retinal degenerations (IRDs) are caused by mutations in over 250 genes that lead to loss of either photoreceptors or RPE and then eventual blindness (Retinal Information Network-RetNet). The mutations alone can lead to vision loss, but it is believed that oxidative stress plays a role in exacerbating the phenotype. The retina is a highly metabolic tissue, producing intrinsic reactive oxygen, but it is also subject to external stimuli (e.g., light, cigarette smoke, diet) that increase the load of reactive oxygen. In the case of IRDs, the cells are already compromised due to the underlying disease–causing mutations, and this may lead to an inability to cope with the reactive oxygen. Oxidative stress is known to cause a wide array of challenges to autophagy, endoplasmic reticulum function, protein folding, and mitochondrial function [10-15]. The effect of oxidative stress on RNA retention/export of known retinal disease–causing genes and genes important for defining the RPE and maintaining proper cell function (herein referred to as RPE markers) has not been studied.

By studying the whole coding transcriptome, with particular emphasis on genes important for maintaining RPE function and those known to contribute to retinal disease, we can determine the role that oxidative stress plays on their retention or export from the nucleus. Using RNA sequencing (RNA-Seq), we show that oxidative stress globally affects RNA localization, and this is especially evident in both RPE markers and retinal disease–causing genes.

METHODS

Culturing of cell lines and differentiation of iPSCs: All reagents were purchased from Invitrogen (Carlsbad, CA) unless noted otherwise. ARPE-19 cells (line APRE-19, ATCC, CRL-2302) were cultured in 49% Advanced DMEM (Fisher Scientific, Pittsburgh, PA, Cat #: 12–491–015), 49% F-12 (Fisher Scientific, Cat #: MT10080CV), and 2% FBS (ATCC, Cat#: 30–2020) and used for RNA-FISH experimentation 24–48 h after reaching confluence. Human induced pluripotent stem cells (iPSC; line ATCC-BXS0114, ATCC, ACS-1028) were seeded at 500,000 cells in a 10-cm dish coated with Matrigel (Corning, Corning, NY). Cells were maintained in TeSR-E8 media (Stem Cell Technologies, Vancouver, Canada) with Rock Inhibitor (Y-27632 dihydrochloride, Santa Cruz Biotechnology, Dallas, TX) at a final concentration of 1 µM/ml. Media without Rock Inhibitor were changed daily. The procedure for differentiating human iPSCs toward RPE was performed as previously described [16,17]. The culture was maintained in RDM until day 80, at which time RPE was dissected and passaged. This process was performed five times to generate the five technical replicates used for this study.

Cell fractionation: Subcellular fractionation was performed as in Rio et al. 2010 with minor adjustments [18]. Briefly, human induced pluripotent stem cell–derived retinal pigmented epithelium (iPSC-RPE) cells were incubated either in RDM media (untreated samples) or in media with 500 µM hydrogen peroxide (treated samples) for 3 h. The treatment conditions (i.e., H_2O_2 concentration and treatment duration) were chosen based on previous evaluations of cell death and oxidative damage analyses in ARPE-19 and human primary RPE cells to minimize cell death before sample collection while still sufficiently invoking oxidative stress [19-25]. Our previous analyses indicating that iPSC-RPE and native RPE are similar from a transcriptional standpoint support the notion that treatment outcomes would be similar in our iPSC-RPE cells [16]. The cells were washed three times with phosphate buffered saline (PBS), incubated at 37 °C for 5 min with TrypLE Express dissociation reagent (Fisher Scientific, Cat#: 12–605–010), and collected via scraping. Cells were pelleted via centrifugation and resuspended in ice-cold cell disruption buffer (10 mM KCl, 1.5 mM $MgCl_2$, 20 mM Tris-HCl [pH 7.5], 1 mM dithiothreitol [DTT, added just before use]). To facilitate swelling, cells were incubated on ice for 20 min then transferred to an RNase-free Dounce homogenizer. Homogenization was achieved using 15–20 strokes of the pestle, and the homogenate was visualized under a microscope to ensure that more than 90% of the cell membranes were sheared, while the nuclei remained intact. Residual cytoplasmic material was separated from the nuclei by adding 0.1% Triton X-100 and mixing gently by inversion. The nuclei were pelleted via centrifugation, and the supernatant (containing the cytoplasmic fraction) was transferred to a new tube. The nuclear pellet was washed in 1 mL ice-cold cell disruption buffer, and both the nuclear and cytoplasmic

fractions were centrifuged. The cytoplasmic supernatant was transferred to a new tube, and the wash was removed and discarded from the nuclear pellet.

RNA isolation: RNA was isolated from the nuclear and cytoplasmic fractions using Tri Reagent (Molecular Research Center Inc., Albany, NY, Cat#: TR 118) following the manufacturer's protocol. After the addition of Tri Reagent, the nuclear and cytoplasmic samples were mixed well by inversion, transferred to phase-lock heavy tubes (VWR, Radnor, PA, Cat#: 10,847-802), and incubated at room temperature for 5 min. Chloroform (200 µl) was added to each sample, followed by vigorous mixing for 15 s and then 15-min incubation at room temperature. Samples were centrifuged, and the aqueous (top) phase transferred to a new 1.5 ml microcentrifuge tube. To remove any contaminating phenol, 400 µl chloroform was added, vigorously mixed, incubated at room temperature for 2 min, and centrifuged. The aqueous phase, containing the RNA, was transferred to a new 1.5 ml microcentrifuge tube. Each volume of RNA solution was then thoroughly mixed with 1/10th volume of 3M sodium acetate, 1 volume of isopropanol, and 2.5 µl RNA-grade glycogen. Samples were incubated at −80 °C for 1 h to precipitate RNA and centrifuged to pellet the RNA, and the supernatant was discarded. To wash the RNA pellets, 75% ethanol was added and then briefly vortexed and centrifuged. Ethanol was removed, and this wash was repeated. Following the second wash, ethanol was removed and pellets were air dried for 5–10 min. RNA was resuspended in 22 µl DNase- and RNase-free water and quantified via nanodrop spectrophotometer. RNA integrity and quality were assessed on a Qubit 4 Fluorometer using a Qubit RNA IQ Assay Kit (Thermo Fisher Scientific, Waltham, MA, Cat#: Q33221). The RNA IQ values all ranged from 7.5 to 8.2, indicating high-quality RNA samples.

RNA library preparation and sequencing: RNA-sequencing libraries were prepared using the SureSelect Strand-Specific RNA Library Prep for Illumina multiplexed sequencing kit (Agilent, Santa Clara, CA, Cat#: G9691A) according to the manufacturer's protocol using 100 ng total RNA, and each sample was indexed for multiplexing. Prior to sequencing, library quality and quantity were determined using High Sensitivity Screen Tape on a TapeStation 4150 (Agilent). Sequencing was performed using a NextSeq 500 (Illumina) generating 2 × 150 bp reads.

Sequencing analysis: Reads were aligned to the human genome (build hg38) with STAR v2.5.2b, and counts were generated for all transcripts in GENCODE v29 using Rsubread v1.32.4 [26-28]. Counts were normalized using reads per kilobase per million reads (RPKM) to examine overall expression. Differential expression analysis using DESeq was performed to determine localization and the effect of treatment [29]. Downstream analyses were performed using custom perl scripts. Heatmaps and Pearson concordance analyses for all samples were generated in R. Pathway analyses were performed using PANTHER with Reactome v65.

RNA-fluorescent in situ hybridization: iPSC-RPE and ARPE-19 cells were seeded onto 8-well chamber slides and 48-well plate coverslips, respectively, and grown to confluence. ARPE-19 cells were chosen for their lack of pigmentation and as a biologic replicate. Cells were prepared using the ViewRNA Cell Plus Assay Kit (Fisher Scientific, Cat#: 88–19000–99) according to the manufacturer's protocol but with the minor alteration of fixation and permeabilization using 3:1 methanol:glacial acetic acid at room temperature. To stain the nuclei, the coverslips were incubated in Hoechst solution. The cells were then mounted and visualized using a Leica TCS SPE confocal microscope, Wetzlar, Germany.

RESULTS

Whole coding transcriptome localization and validation: To examine RNA localization under normal conditions, we generated iPSC-RPE cells using the BXS0114 iPS line (line ATCC-BXS0114, ATCC, Manassas, VA, ACS-93 1028). Nuclear and cytoplasmic RNA was isolated from five technical replicates of each, and RNA-Seq libraries were prepared. Each sample was sequenced on an Illumina NextSeq 500, generating an average of 20 million reads, with 86% of reads aligned to the hg38 human genome build and 92% of these being uniquely aligned. The number of reads was appropriate to sufficiently cover the transcriptome, as indicated by depth of coverage plots (Appendix 1). Concordance analysis revealed only minor variation between the biologic replicates and fraction types (Appendix 2).

Overall, gene expression analysis revealed that approximately one-third of all transcripts were expressed (average RPKM >0.5) in each sample type, with significant overlap between nuclear and cytoplasmic fractions. In total, 76,249 coding transcripts were expressed, 71,086 of which were expressed in the nuclear fraction, and 66,309 in the cytoplasmic fraction. Additionally, to confirm that the iPSC-RPE was sufficiently RPE-like, we examined expression of a comprehensive list of RPE markers originally developed by Liao et al. (2010) [30]. Of the 86 RPE markers, 83 were expressed in the iPSC-RPE (Appendix 3, Appendix 4).

To examine localization, we compared transcript expression in the two fractions and considered a transcript to be localized if it had at least twofold greater expression in one fraction, with an adjusted p value <0.01. If a transcript had a fold-change less than 1.9 in either direction, it was considered

to be mixed localization, regardless of p value. Any transcript not meeting either of these criteria was not assigned a specific localization status. Our analysis identified 3,048 coding transcripts localized to the nucleus, 2,129 to the cytoplasm, and 43,431 that were mixed. (Figure 1A).

RNA fluorescent in situ hybridization (RNA-FISH) is the gold-standard for determining RNA localization [31-33]. Accordingly, we performed RNA-FISH using probes targeted to transcripts that were determined by RNA-Seq to have nuclear (SEC31B, ENST00000492667.5, cyto:nuc expression ratio = 0.015), cytoplasmic (BAX, ENST00000515540.5, cyto:nuc expression ratio = inf.), and mixed (HSD17B4, ENST00000256216.11, cyto:nuc expression ratio = 1.2) localization (Figure 1C and Appendix 5). In all cases, the RNA-FISH results validated the RNA-Seq

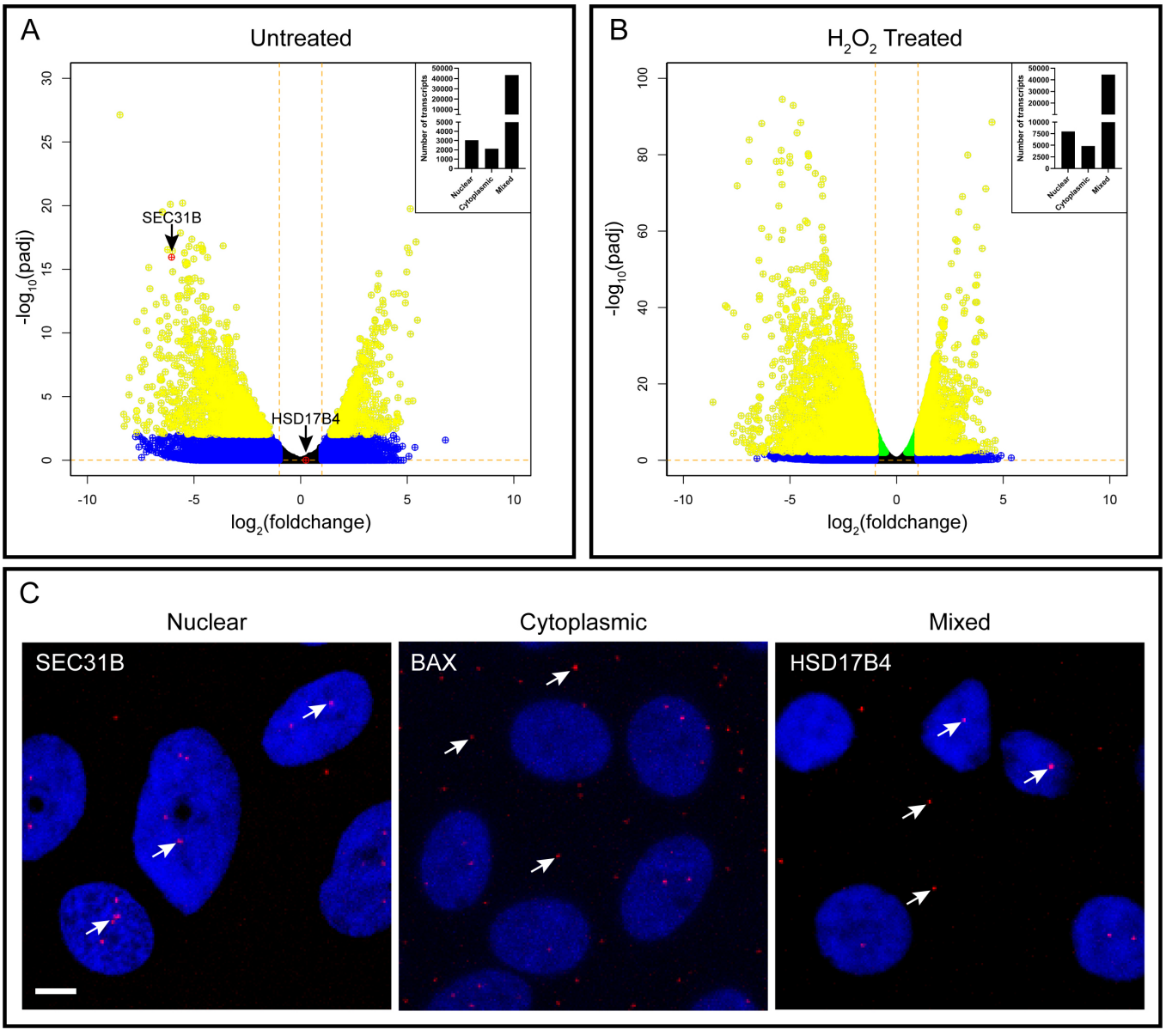

Figure 1. Distribution of coding transcripts in the RPE. Volcano plots of all transcripts in control BXS iPSC-RPE (**A**) and H_2O_2-treated BXS iPSC-RPE (**B**). Log_2 cytoplasm:nuclear fold change and corresponding log_{10} adjusted p value are plotted for each transcript. Transcripts with fold change >2 are colored blue, adjusted p<0.01 are green, and both fold change >2 and adjusted p<0.01 are yellow. Genes confirmed via FISH are red (**A**). Note that BAX is not expressed in the nuclear fraction; hence, it has infinite fold change and is not seen on the plot. (**C**) RNA-FISH images from BXS0114 iPSC-RPE cells confirming localization of SEC31B, BAX, and HSD17B4 (red) and counterstained with Hoechst solution (blue). Arrows indicate some of the localized RNAs. Scale bar is 5 µm.

findings. Additionally, we evaluated contamination between the fractions by comparing the expression of lncRNA transcripts NEAT1 and MALAT1, which are known to be heavily localized to the nucleus. We found that NEAT1 had a DESeq normalized count of 2,415.07 in the nucleus and 34.65 in the cytoplasm. MALAT1 showed similar results with a 278.36 count in the nucleus and 2.68 in the cytoplasm. These data, in combination with the RNA-FISH, demonstrated that minimal cross contamination of the fractions occurred.

Effect of oxidative stress on localization and expression: To determine the influence of oxidative stress on RNA localization, we performed the above experiments following treatment of the iPSC-RPE with 500 µM H_2O_2 for 3 h. H_2O_2 is commonly used in AMD studies to mimic environmental oxidative stressors, which are strong epidemiologic risk factors for AMD progression [34]. We chose the concentration and treatment time from previously used ranges [19-25] to elicit oxidative stress with minimal levels of cell death upon sample collection.

Overall expression analysis in the treated samples revealed similar, albeit slightly lower, numbers compared to the control. In total, 73,669 transcripts were expressed in the H_2O_2-treated line, with 69,294 expressed in the nuclear fraction and 63,581 expressed in the cytoplasmic fraction. Further, we again detected 83 of the 86 RPE markers to be expressed (Appendix 3, Appendix 4).

While overall expression did not significantly change after treatment, we found that H_2O_2 caused a transcriptome-wide increase in localization. Over twice as many transcripts were localized to the nucleus and cytoplasm in the treated line (7,995 and 4,813, respectively), although the number of mixed localization transcripts (44,462) remained similar to that seen in control conditions (Figure 1B). Notably, 2,376 of the nuclear localized and 1,286 of the cytoplasmic localized transcripts were shared between both control and treated conditions (Figure 2). In other words, the majority of transcripts localized to one fraction in the control remained so after peroxide treatment, with 78% of the nuclear and 60% of the cytoplasmic transcripts maintaining their localization after treatment, and we saw an influx of additional localized transcripts after treatment.

To better understand the overall effect on localization resulting from H_2O_2 treatment, we examined the changes in greater detail. In only a few cases did the localization change from cytoplasmic to nuclear, or vice versa, after treatment with H_2O_2. Indeed, only 16 transcripts were localized in one fraction under control conditions and changed to the other fraction after H_2O_2, with 8 moving in each direction (Appendix 6). Slightly more transcripts are localized to one fraction in control samples and classified as mixed after H_2O_2 treatment. We found 150 transcripts to be nuclear localized in the control cells and mixed after treatment and 386 localized to the cytoplasm in control and mixed after treatment. Interestingly, our data suggested that H_2O_2 treatment would result in more defined transcript localization; we saw a fraction of transcripts classified as mixed in control becoming localized after treatment. In other words, transcripts that were roughly equally divided between the nucleus and cytoplasm under control conditions were either more stringently retained in the nucleus or more thoroughly exported to the cytoplasm after treatment. We found 1,104 transcripts moving to nuclear localization and 1,628 moving to cytoplasmic localization, which was evidence of an overall increase in the number of transcripts showing localization after exposure to oxidative stress (Figure 2D, Appendix 7).

We also examined expression changes due to oxidative stress through differential expression analysis using DESeq [29]. We looked at each fraction separately to identify expression changes specific to nuclear or cytoplasmic fractions after treatment, and we considered a transcript to be differentially expressed if it had an adjusted p value <0.01 and greater than twofold expression change. We then grouped differentially expressed transcripts by degree of change, so as to examine the effect of oxidative stress more thoroughly. We found that while a subset of differentially expressed transcripts showed a small degree of change after treatment, most transcripts with significant changes were turned either completely on or off (Figure 3). Our analysis of the nuclear fractions identified 611 coding transcripts significantly changed following H_2O_2 treatment. Of the 318 transcripts upregulated after treatment, 247 were not expressed in the untreated nuclear fractions, and of the 293 transcripts downregulated, 262 showed no expression after treatment. We found slightly fewer transcripts with significantly altered expression after treatment in the cytoplasmic fractions, with a total of 559 coding transcripts showing changes. There were 277 transcripts upregulated after treatment, 202 of which were not expressed in the untreated control cytoplasmic fractions, and 282 transcripts downregulated, with 253 showing no expression after treatment. These data indicated that, regardless of the fraction analyzed and direction of change, most of transcripts with significantly altered expression were turned either on or off completely.

To give greater context to the localization and expression changes observed upon H_2O_2 treatment, we performed Pathway analysis using Reactome groupings. The analysis revealed a broad swathe of pathways overrepresented among transcripts with localization or expression changes after

treatment (Appendix 8, Appendix 9, Appendix 10, Appendix 11, Appendix 12). Interestingly, pathways relating to RNA processing and metabolism featured heavily in these lists. Furthermore, the pathways "cellular responses to external stimuli" and "cellular responses to stress" were found to be overrepresented among both the nuclear and cytoplasmic groups of transcripts whose expression was turned on completely after treatment (Appendix 11, Appendix 12). Curiously, no pathways were found to be overrepresented in the group of transcripts whose expression was turned off completely in response to H_2O_2. Of the transcripts that shifted localization after oxidative stress, three groupings were too small to yield outputs from the analysis: 1) those that moved from nuclear to cytoplasmic upon treatment, 2) those that moved from cytoplasmic to nuclear upon treatment, and 3) those that moved from nuclear to mixed upon treatment.

Specific genes of interest: Given the importance of the RPE to retinal function and disease pathogenesis, we specifically analyzed the localization of three sets of genes: those involved in AMD, those involved in IRDs, and the RPE markers. In all

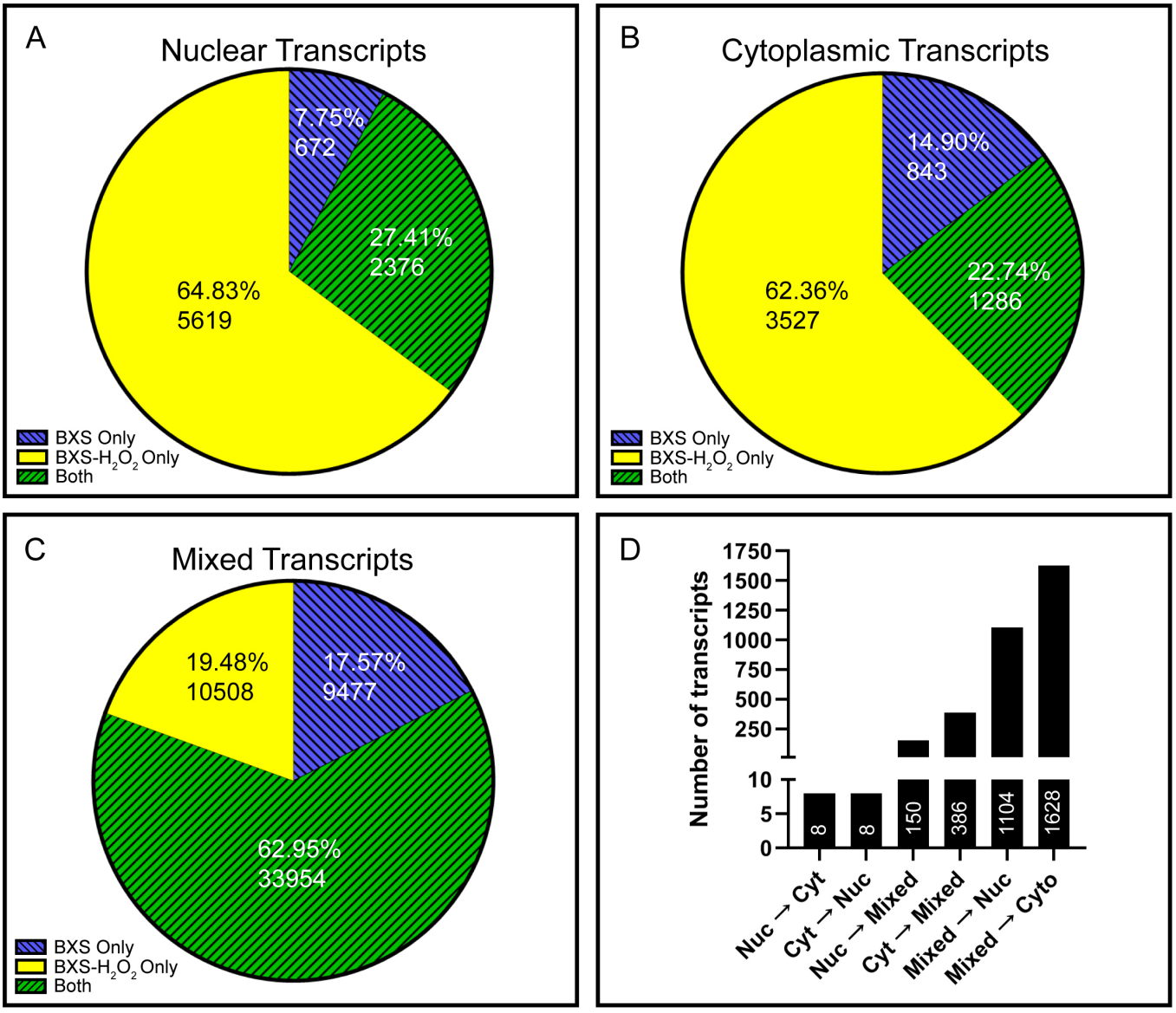

Figure 2. RPE transcript localization is altered by oxidative stress. All transcripts localized to the nucleus (**A**), cytoplasm (**B**), or showing mixed localization (**C**) in control samples (blue), treated samples (yellow), or both (green). Bar graph shows the number of transcripts with altered localization after treatment (**D**). Transitions from control to treated are indicated (e.g., Nuc → Cyt indicates transcripts that are nuclear localized in the control samples and cytoplasmically localized in the treated samples).

three of these gene sets, we saw an increase in overall localization after treatment, with more noticeable changes in the cytoplasmic fraction (Figure 4). The 51 genes with potential involvement in AMD were composed of 853 transcripts. Of these, 51 transcripts were localized to the nucleus and seven to the cytoplasm in control iPSC-RPE. Following treatment, there was a slight increase in the number of transcripts localized to the nucleus (68) and over twice as many localized to the cytoplasm (17). This trend was even more evident in the 2,299 transcripts expressed from 227 IRD genes (RetNet). In these genes, we again saw a notable increase in localization to the nucleus after treatment, with 61 nuclear localized transcripts in the control and 97 after treatment. Moreover, nearly three times as many transcripts were localized to the cytoplasm after exposure to H_2O_2; we found 13 in the control, compared with 36 after treatment. The RPE marker list was partially composed of genes from the other two sets and consisted of 86 genes expressing 958 transcripts. Here, we saw roughly equal numbers of transcripts localized to the nucleus (40 control and 41 treated) but, striking, ten times as many transcripts localized to the cytoplasm in the treated relative to the control (ten control and 97 treated).

Our in-depth analysis of transcripts from these gene lists revealed that the majority of transcripts localized to the nucleus in the control cells were also nuclear localized after treatment (94% AMD, 79% IRD, 78% RPE), while we saw far fewer of the transcripts localized to the cytoplasm in the control continue to localize to the cytoplasm after treatment (14% AMD, 10% IRD, 38% RPE). The increase in cytoplasmic localized transcripts overall, coupled with the fact that few transcripts localized to the cytoplasm in control continued to be similarly localized after treatment, warrants further exploration. As with the whole transcriptome, we found that most of the localization changes in these genes were a result of transcripts that were mixed in control cells moving to cytoplasmic localization after exposure to

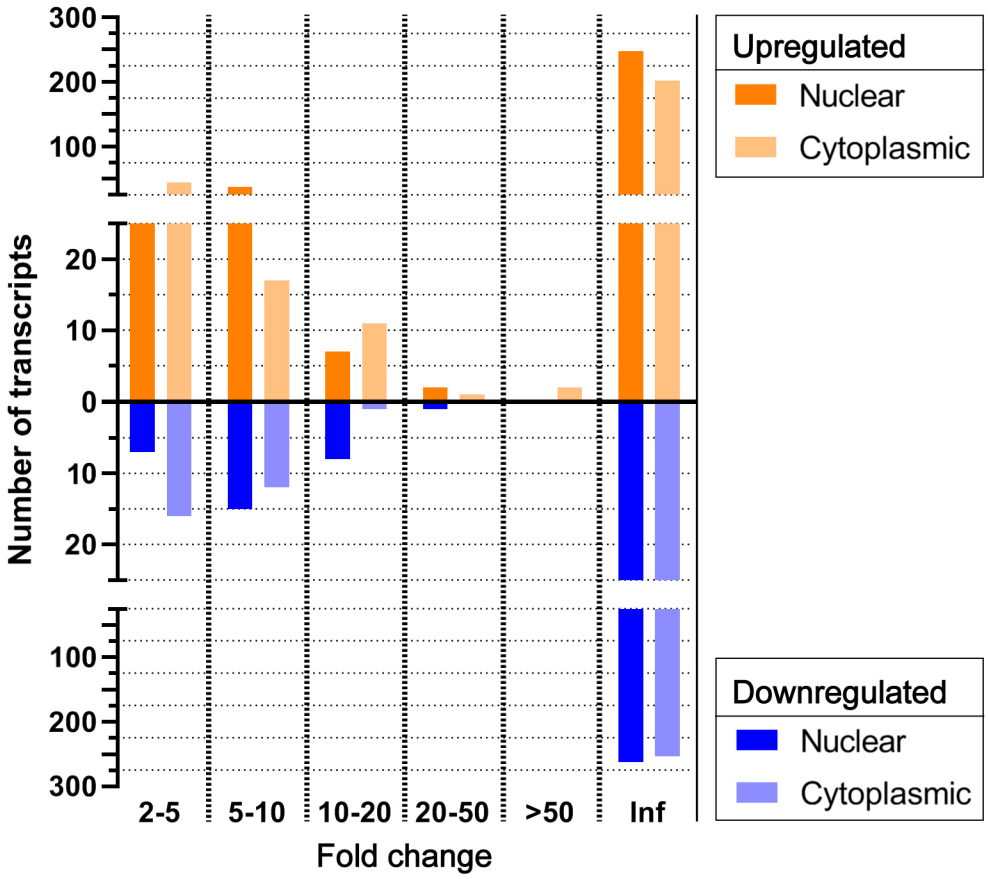

Figure 3. Majority of differentially expressed transcripts are turned on or off by peroxide treatment. Transcripts differentially expressed after peroxide treatment in both nuclear and cytoplasmic fractions. Transcripts are graphed by direction of change and binned by fold change. In both the nucleus and cytoplasm, most DE transcripts are either turned on (have no expression in control) or turned off (have no expression after treatment), as indicated by the infinite (Inf) fold change bin.

H_2O_2. Notably, we saw multiple isoforms from each gene with altered localization. From the set of AMD genes, 12 transcripts from five genes moved from mixed to cytoplasm after treatment, representing 10% of the genes in this list. Of the IRD genes, 23 transcripts from 11 genes shifted localization from mixed to cytoplasm, representing 5% of this list. A full 20% of the RPE gene list showed a shift from mixed to cytoplasmic localization, with 89 transcripts from 18 genes moving in this way. This dramatic shift in transcripts localized to the cytoplasm after H_2O_2 treatment requires more in-depth analysis to determine the potential role these changes may play in the RPE and in AMD and IRD disease pathogenesis.

DISCUSSION

RNA retention in the nucleus is a mechanism for controlling protein abundance in individual cells [1,35-37]. This mechanism affords the cell the ability to quickly respond to changing environmental conditions, as has been shown for heat stress and hypoxia. Conversely, aberrant RNA retention can harm the cell and lead to disease pathogenesis, such as in myotonic dystrophy, Alzheimer disease, and glial cell tumors [3-6]. After conducting a thorough evaluation of the whole coding transcriptome, we found that oxidative stress caused changes in RNA localization, and these changes were especially evident in genes known to cause retinal degeneration.

Interestingly, our data showed mRNA export from the nucleus to be more nuanced than the dogmatic view that mRNA is quickly processed and transported out of the nucleus following transcription. While it is known that some mRNAs undergo processing in addition to capping, splicing, and polyadenylation, and these extra processes will cause retention of the transcript, our data suggested retention of mRNA to be much more ubiquitous than previously understood [38,39]. Specifically, our results contrasted with the findings of Ulitsky et al. (2015) that showed that most mRNA transcripts localize to the cytoplasm in the MIN6 mouse insulinoma pancreatic beta cell line, while only 30% of mRNAs are retained in the nucleus [1]. Further, in control mouse liver cells, they observed 13.1% of mRNAs to be retained in the nucleus. In contrast, we observed roughly 59% of localized transcripts retained in the nucleus in our control iPSC-RPE line, while H_2O_2 treatment led to 62% of localized mRNAs being retained in the nucleus. The differences observed between the two studies can be attributed to multiple factors. First, it is possible, and likely, that different cell types retain and/or export mRNA differently based on their needs. Second, species differences may play a role, as our study was performed in human cells, while that of Ulitsky et al. (2015) was performed in mouse cells. Finally, cell origin could factor into the differences. The MIN6 cell line is derived from cancerous cells, while the liver cells were primary cultures. Reprogramming and differentiation, as was performed for the iPSC-RPE, may introduce variation as well. With respect to gene expression, we have previously shown that while iPSC-RPE are mostly similar to native RPE,

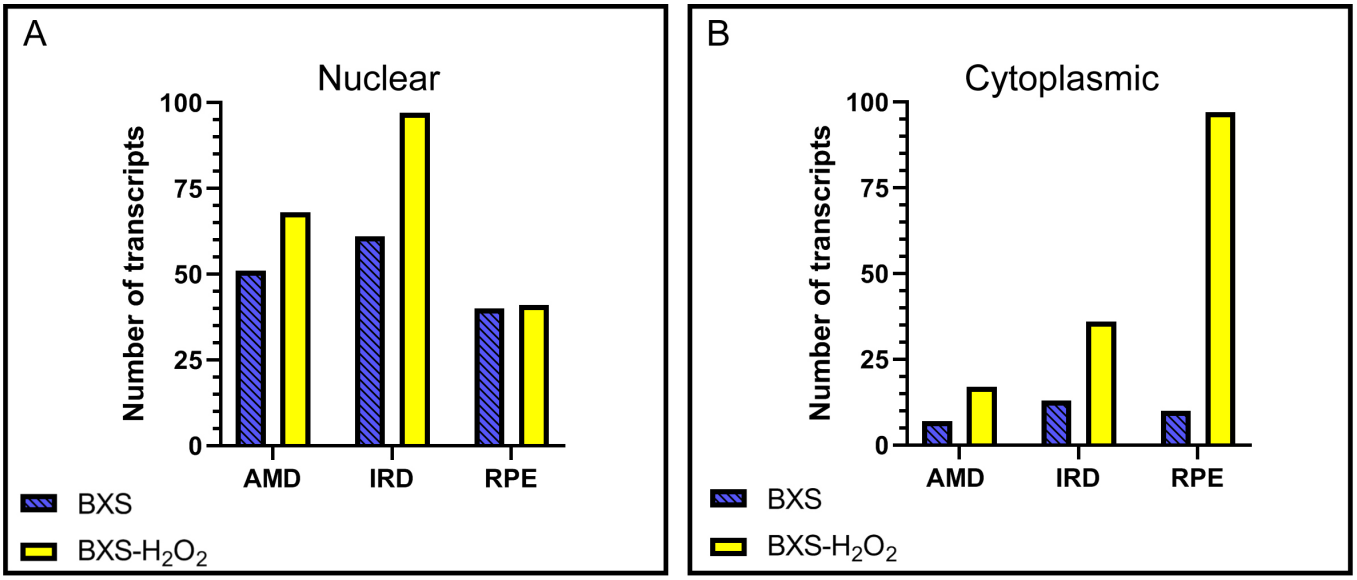

Figure 4. Localization of transcripts involved in AMD and IRDs, as well as RPE marker transcripts. Transcripts involved in AMD, IRDs, and RPE markers that localize to the nucleus (**A**) and cytoplasm (**B**) in control and treated samples.

differences do exist [16]. These differences may carry over to mRNA retention and export.

The mechanisms contributing to the shift in transcript localization in response to H_2O_2 exposure are currently unknown. Although the RNA context (e.g., splicing status, RNA editing) may vary, RNA transcripts are thought to be retained in the nucleus through two mechanisms: 1) binding of retention factors that anchor the transcripts to structural entities within the nucleus (e.g., stalled early spliceosomes, nuclear speckles, paraspeckles, chromatin) and 2) prevention of the transcripts from binding nuclear export factors [2]. Whether and how oxidative stress influences these mechanisms to alter transcript localization is a topic worthy of additional inquiry.

The cellular consequences of RNA retention are situation dependent. For example, under normal environmental and cellular conditions, RNA retention can serve to buffer bursts of transcription as a mechanism to maintain proper protein levels [1-3,37]. Further, retaining excess transcripts in the nucleus can provide flexibility to the cell for rapidly responding to a stressor [8]. On the other hand, abnormal retention and, conversely, abnormal transport to the cytoplasm can lead to cytotoxicity [2,40]. Given the high oxidative load experienced by the retina under normal conditions, we set out to understand the that role oxidative stress has on the localization of genes necessary for proper maintenance and function of the RPE. For example, we found that transcripts for both *IFT172* and *NPHP4* were not exported to the cytoplasm following H_2O_2 treatment. Both genes are involved in cilia formation, like those found in the apical processes of the RPE, and recessive mutations lead to retinitis pigmentosa, among other systemic pathologies. Similarly, *NPLOC4*, which is implicated in AMD risk, was also not exported to the cytoplasm following oxidative stress. On the other hand, export of an isoform of *RGR*, a gene implicated in recessive retinitis pigmentosa, increased after treatment.

It is worth considering the effect that altered RNA localization has on protein production, and this will need to be examined in detail on a gene-by-gene basis. Unfortunately, the acute H_2O_2 exposure of this study does not lend itself to examining such changes, since changes in protein levels lag behind disruptions in RNA production and localization. In addition, many genes have multiple isoforms, which complicates most methods of quantifying protein level changes in response to changes in transcript localization in two ways: 1) each isoform can possess a varied localization pattern, and 2) it is largely unclear which isoforms of a given gene go on to produce proteins [41]. Indeed, future studies will require a longer stress-exposure timescale and a granular approach to determine whether and how the protein levels of particular genes are influenced by shifts in RNA localization.

Nevertheless, the data we have provided did allow us to formulate hypotheses regarding how shifting RNA localization may affect cellular processes. In examining the functions of the 16 transcripts that shifted localization from nuclear to cytoplasmic or vice versa in response to H_2O_2 treatment, there are clues that altered RNA localization may assist in the RPE stress response. FGFR1 and ANXA2, whose transcripts shifted from cytoplasmic to nuclear in response to oxidative stress, both play a role in cell growth and differentiation [42-44]. On the other hand, POLD2 and HIKESHI, whose transcripts shifted from nuclear to cytoplasmic, are important in the recovery from DNA damage and heat shock insults [45-48]. Considering the functions of these proteins, the observed shifts in RNA localization would likely lead to a decrease in cell growth and an increase in repair processes, thus granting the cell time and capacity to resolve the damage caused by the H_2O_2 exposure. Clearly, additional studies will be required to test such a hypothesis and to fully understand the implications of shifting RNA localization in response to stress.

Disease pathogenesis is likely to be a complicated process, and not solely attributable to mutations in a single gene. Rather, it is highly probable that other factors, both internal and external, contribute to disease progression. Our study is the first to evaluate the localization of mRNA in the RPE under a ubiquitous environmental stressor. This work adds to the growing evidence that alters the paradigm of rapid mRNA export from the nucleus. Further, while localization changes of mRNA from disease-causing genes can potentially be implicated in disease progression under oxidative stress, it is also possible that these changes occur to protect the cell. Our data suggest a complicated, multifaceted impact of oxidative stress on altered nuclear retention, with promising potential for a role in RPE homeostasis and retinal disease pathogenesis; nevertheless, future studies are needed to fully explore these possibilities using disease models or primary tissue.

APPENDIX 1. DEPTH OF COVERAGE OF FRACTIONATED RNA-SEQ.

To access the data, click or select the words "Appendix 1." Depth of coverage plots of representative cytoplasmic BXS (A), nuclear BXS (B), cytoplasmic BXS-H_2O_2 (C), and nuclear BXS-H_2O_2 (D) samples.

APPENDIX 2. SUMMARY OF CONCORDANCE BETWEEN SAMPLES.

To access the data, click or select the words "Appendix 2."

APPENDIX 3.

To access the data, click or select the words "Appendix 3." RPE marker expression in control and treated cells. Heatmap showing the expression of 86 RPE marker genes in the nuclear and cytoplasmic fractions of the BXS iPSC-RPE control and H_2O_2-treated samples. In both conditions, 83 of the 86 genes are expressed above RPKM 0.5.

APPENDIX 4. LIST OF RPE MARKER EXPRESSION.

To access the data, click or select the words "Appendix 4."

APPENDIX 5. VALIDATION OF TRANSCRIPT LOCALIZATION IN ARPE-19 CELLS.

To access the data, click or select the words "Appendix 5." RNA-FISH images from ARPE-19 cells confirming localization of SEC31B, BAX, and HSD17B4 (red) and counterstained with Hoechst solution (blue). Arrows indicate some of the localized RNAs. Scale bar is 5 µm.

APPENDIX 6. LIST OF GENES THAT SWITCH LOCALIZATION FROM AFTER PEROXIDE TREATMENT.

To access the data, click or select the words "Appendix 6."

APPENDIX 7. EXPRESSION OF GENES WHOSE TRANSCRIPTS SHIFT LOCALIZATION UPON PEROXIDE TREATMENT.

To access the data, click or select the words "Appendix 7." Heatmaps showing the expression of genes that, upon H_2O_2 treatment, shift from mixed to nuclear localization (A), from mixed to cytoplasmic localization (B), from nuclear to mixed localization (C), and from cytoplasmic to mixed localization (D).

APPENDIX 8. PATHWAY ANALYSIS OF TRANSCRIPTS THAT SHIFT FROM MIXED TO NUCLEAR LOCALIZATION UPON PEROXIDE TREATMENT.

To access the data, click or select the words "Appendix 8."

APPENDIX 9. PATHWAY ANALYSIS OF TRANSCRIPTS THAT SHIFT FROM MIXED TO CYTOPLASMIC LOCALIZATION UPON PEROXIDE TREATMENT.

To access the data, click or select the words "Appendix 9."

APPENDIX 10. PATHWAY ANALYSIS OF TRANSCRIPTS THAT SHIFT FROM CYTOPLASMIC TO MIXED LOCALIZATION UPON PEROXIDE TREATMENT.

To access the data, click or select the words "Appendix 10."

APPENDIX 11. PATHWAY ANALYSIS OF GENES THAT ARE TURNED ON IN THE NUCLEAR SAMPLES UPON PEROXIDE TREATMENT.

To access the data, click or select the words "Appendix 11."

APPENDIX 12. PATHWAY ANALYSIS OF GENES THAT ARE TURNED ON IN THE CYTOPLASMIC SAMPLES UPON PEROXIDE TREATMENT.

To access the data, click or select the words "Appendix 12."

ACKNOWLEDGMENTS

Facilities and resources provided by the VA Western New York Healthcare System to MHF. MHF is also a Research Biologist at the VA Western New York Healthcare System, Buffalo, NY. Computational support was provided by the Center for Computational Research at the University at Buffalo. Next Generation Sequencing services were provided by the Genomics Core at the Children's Hospital Los Angeles. The contents of this manuscript do not reflect those of the Department of Veterans Affairs or the USA Government. **Author Contributions**: TJK and MHF designed the study. TJK and MHF performed experiments. EDA and MHF analyzed and interpreted the data. MHF, EDA, and TJK wrote and edited the manuscript. **Funding**: This work was supported by grants R01EY028553 (NIH/NEI), M2019108 (BrightFocus Foundation), I01 BX004695 (VA Merit/BLR&D Service) to MHF. **Data Availability Statement**: The data sets generated for this study can be found in the GEO REPOSITORY, GEO accession GSE158909.

REFERENCES

1. Halpern KB, Caspi I, Lemze D, Levy M, Landen S, Elinav E, Ulitsky I, Itzkovitz S. Nuclear Retention of mRNA in Mammalian Tissues. Cell Reports 2015; 13:2653-62. [PMID: 26711333].

2. Wegener M, Müller-McNicoll M. Nuclear retention of mRNAs – quality control, gene regulation and human disease. Semin Cell Dev Biol 2018; 79:131-42. .

3. Sergio Comincini Laurent R. Chiarelli, Paola Zelini, Igor Del Vecchio, Alberto Azzalin, Agustina Arias, Valentina Ferrara, Paola Rognoni, Antonella Dipoto, Rosanna Nano, Giovanna Valentini, Luca Ferretti. Nuclear mRNA retention and aberrant doppel protein expression in human astrocytic tumor cells. Oncol Rep 2006; 16:1325-32. [PMID: 17089057].

4. Mastroyiannopoulos NP, Shammas C, Phylactou LA. Tackling the pathogenesis of RNA nuclear retention in myotonic dystrophy. Biol Cell 2010; 102:515-23. [PMID: 20690904].

5. Larkin K, Fardaei M. Myotonic dystrophy—a multigene disorder. Brain Res Bull 2001; 56:389-95. [PMID: 11719277].

6. Sun X, Pan P. Li, Shanshan Zhu, Rachael Cohen, Leonard O Marque, Christopher A Ross, Stefan M Pulst, Ho Yin Edwin Chan, Russell L Margolis, Dobrila D Rudnicki. Nuclear retention of full-length HTT RNA is mediated by splicing factors MBNL1 and U2AF65. Sci Rep 2015; 5:12521-[PMID: 26218986].

7. Mastroyiannopoulos NP, Shammas C, Phylactou LA. Tackling the pathogenesis of RNA nuclear retention in myotonic dystrophy. Biol Cell 2012; 102:515-23. [PMID: 20690904].

8. Zander G, Hackmann A, Bender L, Becker D, Lingner T, Salinas G, Krebber H. mRNA quality control is bypassed for immediate export of stress-responsive transcripts. Nature 2016; 540:593-6. [PMID: 27951587].

9. Lars G. Fritsche, Wilmar Igl, Jessica N Cooke Bailey, Felix Grassmann, Sebanti Sengupta, Jennifer L Bragg-Gresham, Kathryn P Burdon, Scott J Hebbring, Cindy Wen, Mathias Gorski, Ivana K Kim, David Cho, Donald Zack, Eric Souied, Hendrik P N Scholl, Elisa Bala, Kristine E Lee, David J Hunter, Rebecca J Sardell, Paul Mitchell, Joanna E Merriam, Valentina Cipriani. A large genome-wide association study of age-related macular degeneration highlights contributions of rare and common variants. Nat Genet 2016; 48:134-43. .

10. Cui H, Kong Y, Zhang H. Oxidative stress, mitochondrial dysfunction, and aging. Signal Transduct 2012; 2012:646352.-[PMID: 21977319].

11. Bhat AH, Dar KB, Anees S, Zargar MA, Masood A, Sofi MA, Ganie SA. Oxidative stress, mitochondrial dysfunction and neurodegenerative diseases; a mechanistic insight. Biomed Pharmacother 2015; 74:101-10. [PMID: 26349970].

12. Cao SS, Kaufman RJ. Endoplasmic reticulum stress and oxidative stress in cell fate decision and human disease. Antioxid Redox Signal 2014; 21:396-413. [PMID: 24702237].

13. Malhotra JD, Kaufman RJ. Endoplasmic reticulum stress and oxidative stress: a vicious cycle or a double-edged sword? Antioxid Redox Signal 2007; 9:2277-94. [PMID: 17979528].

14. Filomeni G, De Zio D, Cecconi F. Oxidative stress and autophagy: the clash between damage and metabolic needs. Cell Death Differ 2015; 22:377-88. [PMID: 25257172].

15. Kiffin R, Bandyopadhyay U, Cuervo AM. Oxidative stress and autophagy. Antioxid Redox Signal 2006; 8:152-62. [PMID: 16487049].

16. Au ED, Fernandez-Godino R, Kaczynksi TJ, Sousa ME, Farkas MH. Characterization of lincRNA expression in the human retinal pigment epithelium and differentiated induced pluripotent stem cells. Lewin AS, ed. *PLOS ONE*. 2017;12(8):e0183939.

17. Gamm DM, Meyer JS. Directed differentiation of human induced pluripotent stem cells: a retina perspective. Regen Med 2010; 5:315-7. [PMID: 20455642].

18. Rio DC, Ares M, Hannon GJ, Nilsen TW. Preparation of cytoplasmic and nuclear RNA from tissue culture cells. Cold Spring Harb Protoc 2010; 2010:t1554-[PMID: 20516179].

19. Koller A, Bruckner D, Aigner L, Reitsamer H, Trost A. Cysteinyl leukotriene receptor 1 modulates autophagic activity in retinal pigment epithelial cells. Sci Rep 2020; 10:17659-13. [PMID: 33077798].

20. Tohari AM, Alhasani RH, Biswas L, Patnaik SR, Reilly J, Zeng Z, Shu X. Vitamin D attenuates oxidative damage and inflammation in retinal pigment epithelial cells. Antioxidants 2019; 8:341-[PMID: 31450606].

21. Marcia R. Terluk, Mara C. Ebeling, Cody R Fisher, Rebecca J. Kapphahn, Ching Yuan, Reena V. Kartha, Sandra R. Montezuma, Deborah A. Ferrington. N-acetyl-L-cysteine protects human retinal pigment epithelial cells from oxidative damage: implications for age-related macular degeneration. Oxid Med Cell Longev 2019; •••:xxx-.

22. Golestaneh N, Chu Y, Xiao Y-Y, Stoleru GL, Theos AC. Dysfunctional autophagy in RPE, a contributing factor in age-related macular degeneration. Cell Death Dis 2017; 8:e2537-2537. [PMID: 28055007].

23. Deborah A. Ferrington, Mara C Ebeling, Rebecca J Kapphahn, Marcia R Terluk, Cody R Fisher, Jorge R Polanco, Heidi Roehrich, Michaela M Leary, Zhaohui Geng, James R Dutton, Sandra R Montezuma. Altered bioenergetics and enhanced resistance to oxidative stress in human retinal pigment epithelial cells from donors with age-related macular degeneration. Redox Biol 2017; 13:255-65. [PMID: 28600982].

24. Sayak K. Mitter, Chunjuan Song, Xiaoping Qi, Haoyu Mao, Haripriya Rao, Debra Akin, Alfred Lewin, Maria Grant, William Dunn Jr, Jindong Ding, Catherine Bowes Rickman, Michael Boulton. Dysregulated autophagy in the RPE is associated with increased susceptibility to oxidative stress and AMD. Autophagy 2014; 10:1989-2005. [PMID: 25484094].

25. Shimomachi M, Hasan MZ, Kawaichi M, Oka C. HtrA1 is induced by oxidative stress and enhances cell senescence through p38 MAPK pathway. Special Issue: Stem Cells 2013; 112:79-92. [PMID: 23623979].

26. Dobin A, Carrie A Davis FS, Drenkow J, Zaleski C, Jha S, Batut P, Chaisson M, Thomas R. Gingeras. STAR: ultrafast universal RNA-seq aligner. Bioinformatics 2013; 29:15-21. [PMID: 23104886].

27. Harrow J, Frankish A, Jose M. Gonzalez, Electra Tapanari, Mark Diekhans, Felix Kokocinski, Bronwen L Aken, Daniel Barrell, Amonida Zadissa, Stephen Searle, If Barnes, Alexandra Bignell, Veronika Boychenko, Toby Hunt, Mike Kay, Gaurab Mukherjee, Jeena Rajan, Gloria Despacio-Reyes, Gary Saunders, Charles Steward, Rachel Harte, Michael Lin, Cédric Howald, Andrea Tanzer, Thomas Derrien, Jacqueline Chrast, Nathalie Walters, Suganthi Balasubramanian, Baikang Pei, Michael Tress, Jose Manuel Rodriguez, Iakes Ezkurdia, Jeltje van Baren, Michael Brent, David Haussler, Manolis Kellis, Alfonso Valencia, Alexandre Reymond, Mark Gerstein, Roderic Guigó, Tim J Hubbard. GENCODE: the reference human genome annotation for The ENCODE Project. Genome Res 2012; 22:1760-74. [PMID: 22955987].

28. Liao Y, Smyth GK, Shi W. The R package Rsubread is easier, faster, cheaper and better for alignment and quantification of RNA sequencing reads. Nucleic Acids Res 2019; 47:e47-47. [PMID: 30783653].

29. Anders S, Huber W. Differential expression of RNA-Seq data at the gene level–the DESeq package. *Heidelberg, Germany: European Molecular Biology Laboratory (EMBL)*. 2012.

30. Liao J-L, Yu J, Huang K, Hu J, Diemer T, Ma Z, Dvash T, Yang X-J, Gabriel H. Travis, David S Williams, Dean Bok, Guoping Fan. Molecular signature of primary retinal pigment epithelium and stem-cell-derived RPE cells. Hum Mol Genet 2010; 19:4229-38. [PMID: 20709808].

31. Beckman W, Vuist IM, Kempe H, Verschure PJ. Cell-to-cell transcription variability as measured by single-molecule RNA fish to detect epigenetic state switching. In: Epigenome Editing. Springer; 2018:385–393.

32. Alexander SC, Devaraj NK. Developing a Fluorescent Toolbox To Shed Light on the Mysteries of RNA. Biochemistry 2017; 56:5185-93. [PMID: 28671838].

33. Cui C, Shu W, Li P. Fluorescence in situ hybridization: cell-based genetic diagnostic and research applications. Front Cell Dev Biol 2016; 4:89-[PMID: 27656642].

34. Cano M, Thimmalappula R, Fujihara M, Nagai N, Sporn M, Ai LW, Arthur H. Neufeld, Shyam Biswal, James T Handa. Cigarette smoking, oxidative stress, the anti-oxidant response through Nrf2 signaling, and age-related macular degeneration. Vision Res 2010; 50:652-64. [PMID: 19703486].

35. Chin A, Lécuyer E. RNA localization: Making its way to the center stage. *Biochimica et Biophysica Acta (BBA)* - General Subjects 2017; 1861:2956-70. [PMID: 28630007].

36. Kallehauge TB, Robert M-C, Bertrand E, Jensen TH. Nuclear Retention Prevents Premature Cytoplasmic Appearance of mRNA. Mol Cell 2012; 48:145-52. [PMID: 22921936].

37. Stoeger T, Battich N, Pelkmans L. Passive noise filtering by cellular compartmentalization. Cell 2016; 164:1151-61. [PMID: 26967282].

38. Chen L-L, Carmichael GG. Altered nuclear retention of mRNAs containing inverted repeats in human embryonic stem cells: functional role of a nuclear noncoding RNA. Mol Cell 2009; 35:467-78. [PMID: 19716791].

39. Kannanganattu V. Prasanth, Supriya G Prasanth, Zhenyu Xuan, Stephen Hearn, Susan M Freier, C Frank Bennett, Michael Q Zhang, David L Spector. Regulating Gene Expression through RNA Nuclear Retention. Cell 2005; 123:249-63. [PMID: 16239143].

40. Redford-Badwal DA, Stover ML, Valli M, McKinstry MB, Rowe DW. Nuclear retention of COL1A1 messenger RNA identifies null alleles causing mild osteogenesis imperfecta. J Clin Invest 1996; 97:1035-40. [PMID: 8613526].

41. Reixachs Solé M, Eyras E. Uncovering the impacts of alternative splicing on the proteome with current omics techniques. Wiley Interdiscip Rev RNA 2022; 13:e1707-.

42. Grewal T, Wason SJ, Enrich C, Rentero C. Annexins–insights from knockout mice. Biol Chem 2016; 397:1031-53. [PMID: 27318360].

43. Katoh M, Nakagama H. FGF receptors: cancer biology and therapeutics. Med Res Rev 2014; 34:280-300. [PMID: 23696246].

44. Kelleher FC, O'Sullivan H, Smyth E, McDermott R, Viterbo A. Fibroblast growth factor receptors, developmental corruption and malignant disease. Carcinogenesis 2013; 34:2198-205. [PMID: 23880303].

45. Fuchs J, Cheblal A, Gasser SM. Underappreciated roles of DNA polymerase δ in replication stress survival. Trends Genet 2021; 37:476-87. [PMID: 33608117].

46. Imamoto N. Heat stress-induced nuclear transport mediated by Hikeshi confers nuclear function of Hsp70s. Curr Opin Cell Biol 2018; 52:82-7. [PMID: 29490261].

47. Kose S, Furuta M, Imamoto N. Hikeshi, a Nuclear Import Carrier for Hsp70s, Protects Cells from Heat Shock-Induced Nuclear Damage. Cell 2012; 149:578-89. [PMID: 22541429].

48. Tsegay PS, Lai Y, Liu Y. Replication stress and consequential instability of the genome and epigenome. Molecules 2019; 24:3870-[PMID: 31717862].

Articles are provided courtesy of Emory University and the Zhongshan Ophthalmic Center, Sun Yat-sen University, P.R. China. The print version of this article was created on 2 October 2022. This reflects all typographical corrections and errata to the article through that date. Details of any changes may be found in the online version of the article.